Mammographic Parenchymal Patterns as an Imaging Marker of Endogenous Hormonal Exposure:

A Preliminary Study in a High-Risk Population

Dania Daye, BS, Brad Keller, PhD, Emily F. Conant, MD, Jinbo Chen, PhD, Mitchell D. Schnall, MD, PhD, Andrew D. A. Maidment, PhD, Despina Kontos, PhD

Rationale and Objectives: Parenchymal texture patterns have been previously associated with breast cancer risk, yet their underlying biological determinants remain poorly understood. Here, we investigate the potential of mammographic parenchymal texture as a phenotypic imaging marker of endogenous hormonal exposure.

Materials and Methods: A retrospective cohort study was performed. Digital mammography (DM) images in the craniocaudal (CC) view from 297 women, 154 without breast cancer and 143 with unilateral breast cancer, were analyzed. Menopause status was used as a surrogate of cumulative endogenous hormonal exposure. Parenchymal texture features were extracted and mammographic percent density (MD%) was computed using validated computerized methods. Univariate and multivariable logistic regression analysis was performed to assess the association between texture features and menopause status, after adjusting for MD% and hormonally related confounders. The receiver operating characteristic (ROC) area under the curve (AUC) of each model was estimated to evaluate the degree of association between the extracted mammographic features and menopause status.

Results: Coarseness, gray-level correlation, and fractal dimension texture features have a significant independent association with menopause status in the cancer-affected population; skewness and fractal dimension exhibit a similar association in the cancer-free population ($P < .05$). The ROC AUC of the logistic regression model including all texture features was 0.70 ($P < .05$) for cancer-affected and 0.63 ($P < .05$) for cancer-free women. Texture features retained significant association with menopause status ($P < .05$) after adjusting for MD%, age at menarche, ethnicity, contraception use, hormone replacement therapy, parity, and age at first birth.

Conclusion: Mammographic texture patterns may reflect the effect of endogenous hormonal exposure on the breast tissue and may capture such effects beyond mammographic density. Differences in texture features between pre- and postmenopausal women are more pronounced in the cancer-affected population, which may be attributed to an increased association to breast cancer risk. Texture features could ultimately be incorporated in breast cancer risk assessment models as markers of hormonal exposure.

Key Words: Digital mammography; parenchymal texture; hormonal exposure; breast cancer risk.

As new strategies for breast cancer prevention and early detection become available (1,2), it is essential to provide accurate, clinically relevant methods, to identify women at high risk of breast cancer. Although a lot of progress has been made, current approaches still face limitations. Most research to date has focused on identifying women at increased familial risk (ie, BRCA1/2 carriers), which only account for the 5%–10% of incident breast cancers (3). On the other hand, the National Cancer Institute's breast cancer risk assessment tool for the general population, the Gail model, has only modest discriminatory accuracy at the individual level (4). Studies suggest that risk prediction could be improved by incorporating mammographic parenchymal pattern descriptors (5,6). Parenchymal texture features characterize the spatial distribution and structure of the breast tissue pattern (7–10) and could potentially complement the widely used measure of breast density, which is typically captured using coarse measures of the overall percent of mammographically dense tissue in the breast (11). Studies suggest that texture features, particularly in the low spatial frequencies, are strong predictors of cancer risk (12), even when breast density is considered (13).

Mammographic breast density, which is currently the most commonly used parenchymal pattern descriptor, has been identified as a strong independent risk factor for breast cancer (11) and is also shown to correlate with certain modifiable risk factors, such as endogenous cumulative and circulating hormone levels, exogenous hormonal exposure, diet, and body

Acad Radiol 2013; 20:635–646

From the Departments of Bioengineering (D.D.), Radiology (B.K., E.F.C., M.D.S., A.D.A.M., D.K.), and Biostatistics and Epidemiology (J.C.), University of Pennsylvania, 3400 Spruce St., Philadelphia PA 19104. Received September 5, 2012; accepted December 23, 2012. **Address correspondence to:** D.D. e-mail: ddaye@mail.med.upenn.edu

http://dx.doi.org/10.1016/j.acra.2012.12.016

mass index (14–16). Studies suggest that the biological basis of these associations can be mediated through a number of mechanisms that include increased hormonal exposure, prolactin secretion, or the production of growth factors and non–growth factor peptides (17), which may lead to tissue progression from normal growth to hyperplasia to neoplasia (17,18). Over the past decade, novel parenchymal descriptors characterizing the texture of the breast tissue have also emerged as potentially additional breast cancer risk indicators (7,8,10). Yet, although the biological basis of breast density as a risk factor is starting to be elucidated, the biological determinants of parenchymal texture and its association to breast cancer risk are still not well understood.

We previously reported preliminary evidence that mammographic texture features may be associated with hormonal exposure by correlating them to menopause status in a small screening population (19). In this work, we attempt to further characterize our previously reported observations. Specifically, we explore the association between parenchymal texture descriptors and menopause status, which is used here as a surrogate of cumulative endogenous hormonal exposure in two populations of women: a cancer-free and a cancer-affected population. The rationale is that by contrasting the results from these two subpopulations, we may gain further insight on whether such an association could also be affected, or potentially mediated, by an inherent predisposition to a higher risk for breast cancer. In addition, we assess whether parenchymal texture retains an independent association to menopause status when further adjusting for mammographic density as an additional confounder.

As a first step toward understanding the biological basis of mammographic texture, we hypothesize that mammographic texture patterns are associated with endogenous hormonal exposure. Epidemiologic studies provide evidence for the role of endogenous hormones in the development of breast cancer (20,21), and specifically for their effect on tissue aging, as a key breast cancer risk factor (22). For our study, menopause status was used as a surrogate of endogenous hormonal activity, and as with menopause, there is a drastic reduction in the amount of sex hormones produced by the body (23). Identifying differences in parenchymal texture between pre- and postmenopausal women could serve as a proof of concept, indicating that mammographic texture features reflect the effects of cumulative endogenous hormonal exposure on the breast tissue. Our long-term hypothesis is that mammographic parenchymal features could be incorporated into breast cancer risk estimation models to improve individualized breast cancer risk estimation.

MATERIALS AND METHODS

Study Population

Between June 2002 and December 2005, 650 women (age 27–81) had digital mammography imaging as part of a multimodality breast imaging clinical trial completed in our institution. The study compared the diagnostic performance of different digital breast imaging modalities for women with estimated high risk of breast cancer (>25% lifetime Gail/Claus risk), women with recently detected abnormalities (Breast Imaging Reporting and Data System ≥4 or positive biopsy), and follow-up of previous cancer patients. Women in this trial were volunteers and have signed informed consent. As part of their participation, the women provided demographic and health and reproductive history information. The number of first-degree relatives with breast cancer, number of benign biopsies, age at menarche and age at first live birth, and the woman's race were used to calculate lifetime and 5-year Gail breast cancer risk (4). Exclusion criteria consisted of being pregnant, having a contraindication for magnetic resonance imaging, prior history of cancer in the ipsilateral breast within the last 5 years, being treated with preoperative adjuvant therapy, having a blood sugar level above 200 mg/dL, and having moderate to severe renal disease.

For our study reported here, 297 women were included. To be selected for our study, women had to have digital mammography images available with sufficient image quality, be pre- or postmenopausal, and have no or unilateral breast cancer. Of the 650 women originally enrolled in the multimodality imaging trial, 466 had digital mammography images with no artifacts (eg, biopsy clips) that could potentially confound image analysis. Of those, 169 women were further excluded for one or more of the following: 1) being perimenopausal, 2) having bilateral breast cancer, 3) failing to report: age, estrogen therapy use, contraceptive therapy use, or age at menarche; or 4) having a lesion specifically within the retroareolar region. Of the remaining 297 women included in our study, 143 had unilateral breast cancer (ie, referred here as our cancer-affected population) and 154 had no diagnosis of breast cancer (ie, our cancer-free population). Menopause status was ascertained from completed study questionnaires where participating clinicians indicated whether the woman was premenopausal, postmenopausal, perimenopausal, or had an unknown menopause status. Of the cancer-affected women, 73 women were premenopausal and 70 were postmenopausal. Of the cancer-free population, 88 women were premenopausal and 66 were postmenopausal. Several factors known to affect hormonal levels were also examined, including current estrogen therapy use, current oral contraceptive use, age at menarche, parity, and age at first birth. A summary of the demographic characteristics of the study population is shown in Table 1.

Image Dataset

Bilateral craniocaudal (CC) digital mammography (DM) images were retrospectively analyzed under the Health Insurance Portability and Accountability Act and institutional review board approval. DM acquisition was performed with a GE Senographe 2000D full-field DM system (GE Healthcare, Chalfont St. Giles, UK). The raw x-ray projections were acquired with a spatial resolution

TABLE 1. Characteristics of Our Study Population

	Cancer-Free Women		Cancer-Affected Women	
	Premenopausal	Postmenopausal	Premenopausal	Postmenopausal
Total number	88	66	73	70
Mean age (years)	44.41 ± 7.78	52.39 ± 18.32	45.43 ± 6.02	62.77 ± 7.59
Gail 5-year risk (%)	1.51 ± 1.28	2.85 ± 1.99	1.03 ± 0.70	1.81 ± 0.96
Gail lifetime risk (%)	17.63 ± 8.38	17.62 ± 10.89	12.11 ± 5.18	10.22 ± 4.97
Ethnicity				
Caucasian	76 (87%)	51 (77%)	59 (81%)	54 (77%)
African American	7 (8%)	8 (12%)	8 (11%)	13 (20%)
Asian	2 (2%)	2 (3%)	2 (3%)	1 (1%)
Mixed	1 (1%)	1 (2%)	1 (1%)	1 (1%)
Other, not available	2 (2%)	4 (6%)	3 (4%)	1 (1%)
Estrogen therapy				
Yes	1 (1%)	3 (5%)	1 (1%)	2 (3%)
No	87 (99%)	63 (95%)	72 (99%)	68 (97%)
Contraceptive use				
Yes	2 (2%)	0 (0%)	6 (8%)	0 (0%)
No	86 (98%)	66 (100%)	67 (92%)	70 (100%)
Mean age at menarche (years)	12.57 ± 1.71	12.45 ± 2.74	12.59 ± 1.16	12.33 ± 1.49
Mean age at first birth (years)	27.32 ± 5.68	25.59 ± 6.47	28.40 ± 5.09	24.27 ± 5.33
Parity				
Yes	55 (63%)	56 (85%)	55 (75%)	59 (84%)
No	33 (37%)	10 (15%)	18 (25%)	11 (16%)

of 0.1 mm/pixel and a 16-bit per pixel gray-level depth. Image postprocessing was performed with the GE PremiumView algorithm (24). For cancer-affected women, the unaffected breast was analyzed as a surrogate of inherent healthy breast tissue properties. For the cancer-free women, side-matching was performed to select a similar proportion of left and right breasts as the cancer-affected women. Based on this, the final dataset included 73% right breasts and 27% left breasts.

Parenchymal Texture Analysis

In this study, we implemented gray level cooccurrence matrix–based texture features as well as a number of parenchymal texture descriptors that explore local gray-level patterns in the mammographic images. To extract these descriptors, retroareolar 2.5-cm^2 regions of interest (ROI) were first segmented from the PremiumView postprocessed images using validated automated software (24,25). Briefly, the software implements an edge detection algorithm based on the Hough transform to detect the chest wall in the image (26). Then, the nipple location is detected as the edge point that is furthest perpendicularly from the chest wall, and a 2.5-cm^2 retroareolar ROI is automatically segmented behind the detected nipple. The resulting ROI is in the central breast region and was specifically selected because it typically includes the most dense and texturally complex region of the breast as previously described by Huo et al (8) and provides the most discriminative texture features for differentiating women at high versus low-risk for breast cancer (24,27). Representative retroareolar ROIs from pre- and postmenopausal women are shown in Figure 1.

Texture features of skewness, coarseness, contrast, gray-level correlation, fractal dimension, homogeneity, and energy were computed from each ROI. These features have been previously proposed for general image analysis applications (28,29) and have also been specifically shown to correlate with breast cancer risk when computed from mammographic images (7,8,10,11,24,27,30). Their previous correlation with breast cancer risk suggests their potential to capture, even partially, underlying biological processes in breast tissue. While the exact underlying biologic phenotypes of these reported patterns are not yet fully understood, these features essentially quantitatively explore local patterns in the images based on statistical descriptors. The detailed mathematical derivations are included in the Appendix. Briefly, skewness reflects the asymmetry in the gray-level pixel value distribution, and has been shown to reflect local parenchymal density properties (31,32). Coarseness is a measure of smoothness of image texture and within our context reflects local granularity in parenchymal pattern; its computation is based on the neighborhood gray tone difference matrix (31,32). Contrast, energy and homogeneity, as originally proposed by Haralick (33), reflect local differences in the distribution of image intensity and require the computation of the gray-level spatial co-occurrence matrix. Contrast quantifies variation in image intensity between neighboring pixels; energy is a measure of texture uniformity of the gray-level spatial distribution; and homogeneity reflects the heterogeneity of texture patterns.

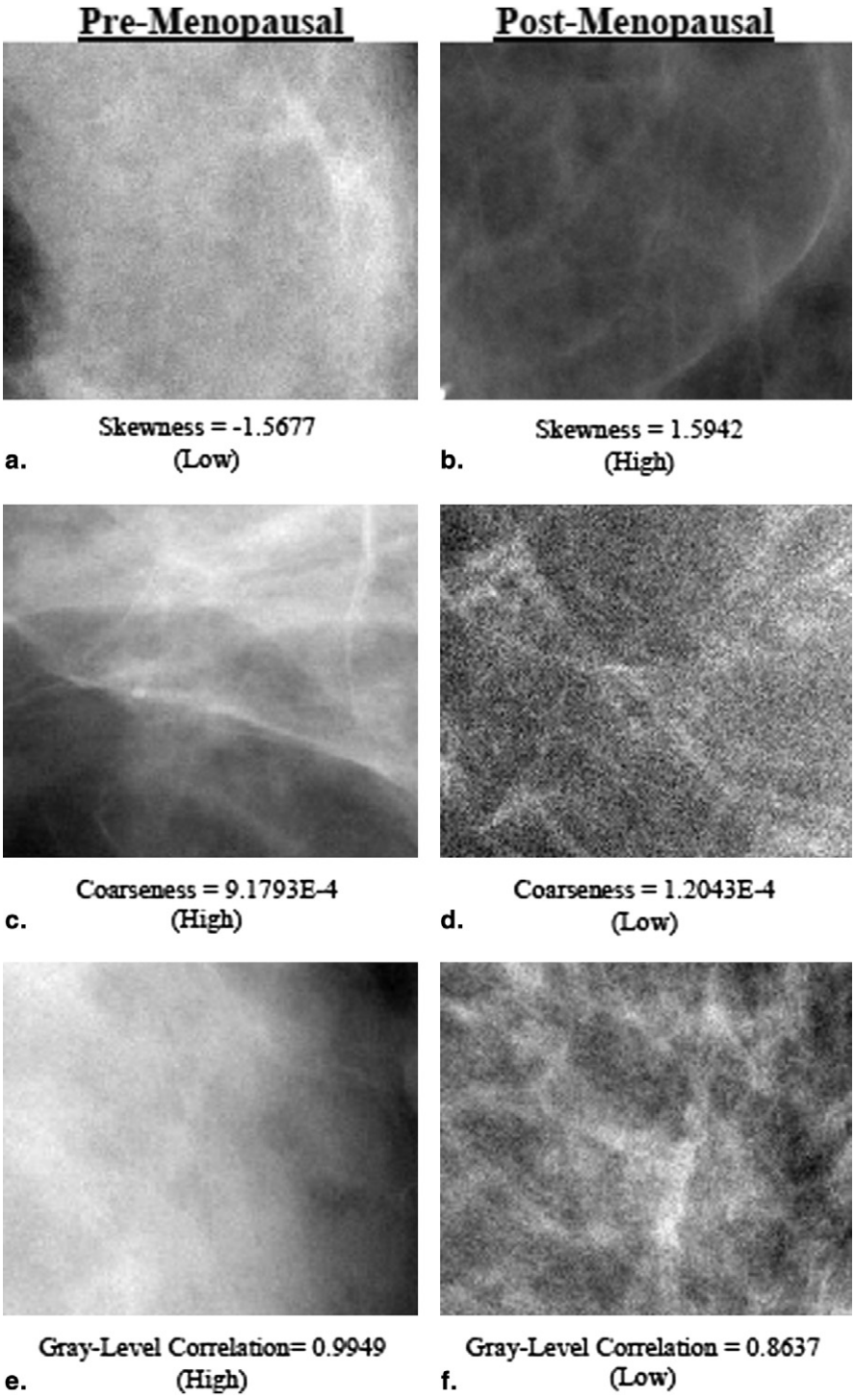

Figure 1. Representative retroareolar regions of interest (ROI) from craniocaudal (CC) mammographic images of unaffected breasts of cancer-affected and cancer-free women. **(a, c, e)** Premenopausal cases. **(b, d, f)** Postmenopausal cases. **(a–f)** ROIs with low skewness (skewness = −1.5677), high skewness (skewness = 1.5942), high coarseness (coarseness = 9.1793E-4), low coarseness (coarseness = 1.2043E-4), high gray-level correlation (gray-level correlation = 0.9949), and low gray-level correlation (gray-level correlation = 0.8637) texture features, respectively. In general, premenopausal women tend to have denser breast parenchyma with smoother texture; postmenopausal women have less dense parenchyma with sharper textures. These characteristics were quantitatively characterized using the implemented texture features. Shown are texture features that exhibited statistically significant differences between pre- and postmenopausal women.

Finally, fractal dimension, computed here using the power spectrum of the Fourier transform (7), indicates the degree of intrinsic self-similarity of the parenchymal pattern at different image resolutions.

Mammographic Density Estimation

Mammographic percent density (MD%) was estimated using previously published validated computer software (34,35). In summary, the computer algorithm first identifies the air–breast boundary via automated thresholding based on edge detection, and the pectoral muscle region, when present, is excluded using a straight line Hough transform (34). Adaptive *k*-class fuzzy-c-means clustering is then performed within the segmented breast region to partition the breast area into multiple clusters of similar grey-level image intensity. A linear classifier is subsequently applied to label the detected subregions into dense tissue versus fat and segment the total dense tissue

area within the breast. MD% is then estimated per standard practice (11) as the percentage of the total breast area occupied by the segmented dense tissue.

Data Analysis

Statistical analysis was performed separately for the cancer-affected and the cancer-free women to account for potential inherent differences in parenchymal tissue properties. For each feature and MD%, we report the mean, standard deviation, coefficient of variation, and intraclass correlation. The intraclass correlation was computed using the left and right breast features of the same woman within each class. Student's *t*-test was performed to assess differences in the means between the pre- and postmenopausal women. To assess interfeature correlation, the Spearman correlation coefficient *r* was computed between each feature pair. To determine the association between texture features, MD%, and menopause status, univariate and multivariate logistic regression analysis was performed (Stata/IC 12, Stata Corp.).

We first investigated the association between each of the texture features independently as well as mammographic density, with menopause status using univariate logistic regression with menopause status as the outcome variable. These univariate models were further adjusted for mammographic density and the potential hormonal confounders to assess the independent contribution of each of the texture feature in association to menopause status.

To assess the collective association between combinations of the texture features and menopause status, multivariate logistic regression was performed using all the computed texture features as explanatory variables. Similarly to univariate analysis, we assessed whether texture features were independently predictive of menopause status after adjusting for mammographic density and the potential hormone-related confounding factors, age at menarche, ethnicity, contraception pill use, hormonal replacement therapy (HRT), parity, and age at first birth. Age at menarche was included as a continuous variable and ethnicity as a categorical variable with five categories as summarized in Table 1. Contraceptive use and HRT use were treated as binary variables. Parity and age at first birth were coded as a single, nominal variable in which 0 referred to nulliparity, 1 to having a first birth before age 30, and 2 referred to having a first birth after age 30.

To alleviate the effect of feature multicolinearity, backward stepwise feature selection was performed in the multivariable models, with a feature entry *P* value of .05 and feature removal *P* value of .1. In all models, estimated logistic regression coefficients were computed and the Wald test was performed to assess significance of the association between each predictor and menopause as the response variable at a 0.05 significance level. To determine the degree of the observed associations, the area under the curve (AUC) of the receiver operating characteristic (ROC) curve was computed for each model to evaluate discriminatory capacity between pre- and postmenopausal status (Matlab V.2012a, Mathworks, Inc., Precision Recall Curve Toolbox) (36). The different ROC AUCs were compared using the bootstrapping test for significance (37). In all analyses, two levels of significance were considered, $P < .05$ as a standard level and $P < .001$ as a more stringent criterion, to account for the multiple tests performed.

RESULTS

Fractal dimension and skewness were statistically significantly different between pre- and postmenopausal women in the cancer-free population (Table 2). Coarseness, gray-level correlation, and fractal dimension were different between the two groups in the cancer-affected population. Representative ROIs illustrating some of these differences are shown in Figure 1. Mammographic density was statistically significantly lower in postmenopausal women in both the cancer-free and cancer-affected populations. Interfeature correlations ranged from low to high ($|r_{min}| = 0.01$, $|r_{max}| = 0.99$) for the different texture features (Table 3). Mammographic density had little to moderate correlation with the extracted texture features ($|r_{min}| = 0.01$, $|r_{max}| = 0.45$).

Univariate logistic regression showed that a number of texture features as well as mammographic density are significantly different between pre- and postmenopausal women (AUC > 0.50; $P < .05$) for both cancer-affected and cancer-free women (Table 4). Skewness and fractal dimension are significantly associated with menopause status in cancer-free women (AUC > 0.50, $P < .05$). Coarseness, gray-level correlation and fractal dimension are significant in cancer-affected women (AUC > 0.50, $P < .05$). After adjustment for MD% and hormonal confounders, fractal dimension maintains significant association with menopause status in the cancer-free population. Coarseness, gray-level correlation, and fractal dimension maintain significance in the cancer-affected population. Mammographic density has the highest univariate AUC of all texture features in both the cancer-free and cancer-affected women (AUC > 0.70). ROC curves with AUC > 0.5 and $P < .05$ were considered as statistically significant.

In multivariate analysis, for the cancer-free women, the multivariable logistic regression model that included all the texture features yielded one significant texture feature coefficient: fractal dimension ($P < .05$) (Table 5). ROC analysis after backward feature selection on the model that included only the texture features yielded an AUC of 0.63 (Fig 2a). The corresponding logistic regression model for the cancer-affected women yielded three significant texture features coefficients: contrast, homogeneity, and skewness ($P < .05$) (Table 5). Following feature selection, ROC analysis on the model that included only the texture feature yielded an AUC of 0.70 (Fig 2b). After adjustment for MD%, fractal dimension maintained significant association with menopause status in the cancer-free women and contrast and homogeneity retained significance in cancer-affected women ($P < .05$); MD% was statistically significant in all models across populations ($P < .05$) (Table 5). After feature selection, ROC curve analysis yielded an AUC of

TABLE 2. Summary of Texture Feature Characteristics in Cancer-Free and Cancer-Affected Women

	Premenopausal				Postmenopausal			
	Mean	SD	CV	ICC	Mean	SD	CV	ICC
Cancer-free population								
Coarseness	4.139E-4	1.688E-4	0.40	0.68	4.498E-4	2.898E-4	0.43	0.66
Contrast	3.528E2	107.05	0.31	0.87	3.443E2	89.459	0.26	0.77
Gray level correlation	9.655E-1	3.450E-2	0.03	0.39	9.658E-1	3.470E-2	0.03	0.71
Energy	8.697E-5	3.054E-5	0.36	0.42	7.874E-5	3.327E-5	0.42	0.67
Homogeneity	1.379E-1	1.370E-2	0.07	0.90	1.384E-1	1.280E-2	0.07	0.91
Fractal dimension*	2.556	0.251	0.10	0.71	2.669	0.163	0.06	0.65
Skewness*	−1.882E-1	0.527	−2.79	0.52	−1.30E-2	0.559	−55.00	0.27
MD (%)**	43.72	15.36	0.34	0.80	34.57	15.37	0.42	0.66
Cancer-affected population								
Coarseness*	4.705E-4	1.617E-4	0.34	0.44	4.085E-4	1.754E-4	0.44	0.63
Contrast	3.266E2	1.609E1	0.49	0.09	3.444E2	1.006E1	0.29	0.68
Gray level correlation*	9.751E-1	2.000E-2	0.02	0.35	9.574E-1	4.200E-2	0.043	0.80
Energy	8.217E-5	3.370E-5	0.41	0.63	9.955E-5	5.575E-5	0.59	0.73
Homogeneity	1.440E-1	1.340E-2	0.07	0.56	1.396E-1	1.220E-2	0.09	0.81
Fractal dimension*	2.658	0.210	0.08	0.59	2.591	0.176	0.07	0.62
Skewness	−0.855E-1	1.166	−13.00	0.07	0.0934	0.492	5.56	0.31
MD (%)**	44.61	14.96	0.33	0.76	33.36	14.09	0.46	0.73

CV, coefficient of variation; ICC: intra-class correlation; MD, mammographic density; SD, standard deviation.
*$P < .05$, **$P < .001$. P values are from t-test comparing differences in feature means between pre- and postmenopausal women.

TABLE 3. Interfeature Spearman Correlation Coefficients in Cancer-Free and Cancer-Affected Women

	Coarseness	Contrast	Gray-Level Correlation	Energy	Homogeneity	Fractal Dimension	Skewness	MD
Cancer-free population								
Coarseness	1.00							
Contrast	−0.44**	1.00						
Gray-level correlation	0.91**	−0.29**	1.00					
Energy	−0.73**	−0.22*	−0.72**	1.00				
Homogeneity	0.47**	−0.99**	0.32**	0.20*	1.00			
Fractal dimension	0.61**	−0.41**	0.52**	−0.30**	0.41**	1.00		
Skewness	0.01	−0.12	−0.15	0.11	0.15	0.12	1.00	
MD (%)	0.09	−0.15	0.16*	0.01	0.13	−0.09	−0.34**	1.00
Cancer-affected population								
Coarseness	1.00							
Contrast	−0.35**	1.00						
Gray level correlation	0.95**	−0.31**	1.00					
Energy	−0.77**	−0.20*	−0.76**	1.00				
Homogeneity	0.34**	−0.93**	0.29**	0.24*	1.00			
Fractal dimension	0.58**	−0.24*	0.54**	−0.42**	0.20*	1.00		
Skewness	−0.20*	0.01	−0.35**	0.29**	0.05	−0.02	1.00	
MD (%)	0.13	−0.18*	0.23*	−0.05	0.17*	0.09	−0.45**	1.00

MD, mammographic density.
*$P < 0.05$, $P < .001$.

0.72 for the cancer-free population (Fig 2c) and an AUC of 0.76 (Fig 2d) for the cancer-affected population.

Further adjustment for age at menarche, ethnicity, contraception use, estrogen therapy use, parity, and age at first birth did not show statistical significant association between any of these potential hormonal confounders and menopause status, for either cancer-free or cancer-affected women, whereas the previously selected texture features and MD% retained significant independent association with menopause status ($P < .05$) (Table 5). All reported models were statistically significant (model P value $< .05$) (Table 5). Although the addition of MD% to the multivariable texture feature models led to a stronger association with menopause status, as indicated by an increase in the ROC AUC of all corresponding models

TABLE 4. Univariate Logistic Regression and ROC Curve Performance in Distinguishing between Pre- and Postmenopausal Women for Each of the Texture Features Alone and after Adjusting for Density and Hormonal Factors

	Texture Feature		Texture Feature + Density		Texture Feature + Density + Hormonal Factors	
	Regression Coefficient	AUC	Regression Coefficient	AUC	Regression Coefficient	AUC
Cancer-free population						
Coarseness	1200	0.55	1600	0.70**	1700	0.71**
Contrast	−0.001	0.50	−0.002	0.71**	−0.002	0.72**
Gray level Correlation	1.80	0.51	4.70	0.70**	4.10	0.70**
Energy	−5700	0.56	−5200	0.70**	−5400	0.70**
Homogeneity	5.20	0.50	13	0.70**	13.10	0.71**
Fractal Dimension	2.30*	0.62*	2.20*	0.71**	2.10*	0.73**
Skewness	0.62*	0.58*	0.24	0.70**	0.27	0.71**
MD (%)	—		−0.05**	0.70**	−0.05**	0.71**
Cancer-affected population						
Coarseness	−2500*	0.64*	−2600*	0.75**	−2600*	0.77**
Contrast	0.0010	0.57	0.0004	0.73**	0.0008	0.76**
Gray level Correlation	−24.00*	0.66**	−23.00*	0.76**	−24.00*	0.78**
Energy	7700	0.59	1100*	0.74**	8800	0.77**
Homogeneity	−25.00	0.57	−18.00	0.74**	−29.00	0.77**
Fractal dimension	−1.90*	0.61*	−2.40*	0.75**	−2.60*	0.78**
Skewness	0.33	0.67	0.05	0.74**	0.03	0.76**
MD (%)	—		−0.05**	0.72**	−0.06**	0.76**

AUC, area under the curve; MD, mammographic density; ROC, receiver operating characteristic.
*P < .05, **P < .001. Asterisk notation on AUC reflects overall P value of regression model.

for both cancer-free and cancer-affected women, assessment of those differences with bootstrapping (37), as compared to the density-only and texture-only models, did not reveal statistical significance (Fig 2).

DISCUSSION

Mammographic parenchymal patterns, traditionally described by breast density, have been strongly associated with the risk of breast cancer (6,33). Recent data suggest an increasing role of additional parenchymal descriptors, such as mammographic texture features, in breast cancer risk assessment (7,8,10,11,24,27,30). Li et al have assessed various computer-extracted mammographic texture features of BRCA1/BRCA2 carriers and women at lower risk of breast cancer (8,10,31,32), showing that parenchymal texture features can identify women at high risk of breast cancer because of genetic predisposition. When applied to the general population, studies also support that mammographic texture analysis could be used in breast cancer risk assessment (11,12,30). Although this evidence suggests an association between mammographic texture and breast cancer risk, the underlying biological basis for this association is still not well understood.

Endogenous hormonal activity, reflected by both cumulative and circulating hormone levels, is strongly associated with increased breast cancer risk and is known to affect the breast tissue (17,22). Mammographic density is heavily affected by hormonal exposure (15,16,18,38) and it is shown to increase with HRT (39) and decrease with menopause (40) and Tamoxifen use (41). Although studies have investigated the effect of hormonal exposure on mammographic density, there are limited data on the effect of hormone-related processes on parenchymal tissue texture. Studies have shown that mammographic texture features are only moderately correlated with density (12) and may be different within the dense versus fatty areas of the breast tissue (42). A study by Raundahl et al (43) showed that computer-extracted mammographic pattern descriptors, including the heterogeneity of the local breast tissue structure, can capture the effect of hormone related interventions, such as HRT.

The underlying biological determinants of parenchymal texture have not been previously explored. Our data suggest that certain mammographic textures features are different between pre- and postmenopausal women. These results indicate that hormonal exposure might have a detectable effect on the texture of the breast tissue, here quantitatively characterized using computerized features. Some of these features, such as fractal dimension, contrast, and homogeneity, maintain a significant association to menopause status even after adjusting for breast density and hormonally related factors, including age at menarche, estrogen treatment, ethnicity, contraceptive use, parity, and age at first birth. In our study, mammographic density has the strongest univariate association to menopause status. When considered in conjunction with texture features in multivariable analysis, the collective association to menopause status is stronger, although not statistically significantly different. Although it is reasonable to assume that

TABLE 5. Logistic Regression Results for Each Partial Regression Coefficient before and after the Addition of Density and Hormonal Variables to the Multivariable Texture Feature Models

	Texture Only		Texture + Density		Texture + Density + Hormonal Factors	
	Regression Coefficient	*P* Value	Regression Coefficient	*P* Value	Regression Coefficient	*P* Value
Cancer-free population						
Model constant	20	.15	20	.19	23	.13
Coarseness	920	.65	1400	.50	1600	.48
Contrast	−0.01	.28	−0.01	.17	−0.01	.14
Gray-level correlation	−15	.18	−8.35	.51	−11	.40
Energy	−5700	.73	4200	.98	−2100	.91
Homogeneity	−76	.27	−98	.18	−100	.17
Fractal dimension	3.30	<.01	2.68	.04	2.60	.04
Skewness	0.48	.15	0.18	.60	0.19	.59
MD (%)			−0.05	<.01	−0.05	<.01
Age at menarche					0.01	.92
Estrogen therapy					0.90	.49
Contraceptive use					0.49	.71
Ethnicity					0.02	.49
Parity/age at first birth					0.45	.104
Model *P* value	.017		<.001		<.001	
Cancer-affected population						
Model constant	39	.01	37	.02	44	.01
Coarseness	3200	.15	2500	.27	330	.17
Contrast	−0.01	<.01	−0.01	.04	−0.01	.04
Gray-level correlation	−24	.12	−24	.15	−29	.11
Energy	10,000	.12	10,000	.17	9400	.21
Homogeneity	−95	<.01	−65	.04	−78	.03
Fractal dimension	−0.62	.61	−1.01	.43	−1.20	.38
Skewness	0.99	.02	0.56	.19	0.56	.22
MD (%)			−0.04	<.01	−0.03	<.01
Age at menarche					0.04	.79
Estrogen therapy					−1.00	.48
Contraceptive use					−1.60	.178
Ethnicity					0.07	.433
Parity/age at first birth					−0.46	.142
Model *P* value	<.001		<.001		<.001	

MD, mammographic density.

P values are shown for the Wald test for each partial regression coefficient and for overall model significance.

mammographic texture and density may have some common biological determinants, the independent significant association of certain texture features to menopause status after adjusting for density suggests that these features may reflect additional information related to the effect of endogenous hormonal activity on the breast tissue. This is also supported by the low correlation observed between mammographic density and the texture features used in our study. Combined, these results suggest that parenchymal texture might provide complementary information in addition to mammographic density in reflecting the effects of endogenous hormonal exposure of the breast tissue, a known risk factor of breast cancer.

Our results indicate that, in both univariate and multivariate analysis, the association between texture features and menopause status may be higher in cancer-affected compared to cancer-free women, suggesting that the potential effect of cumulative endogenous hormonal exposure on the breast tissue may be more pronounced for women who ultimately develop breast cancer. This hypothesis is supported by the initial hypothesis posed by Pike (22) that endogenous hormonal exposure has an effect on the breast tissue aging processes and that increased cumulative hormonal exposure is related to a higher risk for developing breast cancer. These results may be of significance because texture features could ultimately be used as imaging markers of endogenous hormonal exposure and therefore as imaging markers of cancer risk. In our study, this reported effect, however, could be confounded by the higher mean age of the postmenopausal women in our cancer-affected population compared to the same group in the cancer-free population, which in turn could correspond to a longer period of endogenous hormonal exposure. Also of note, different

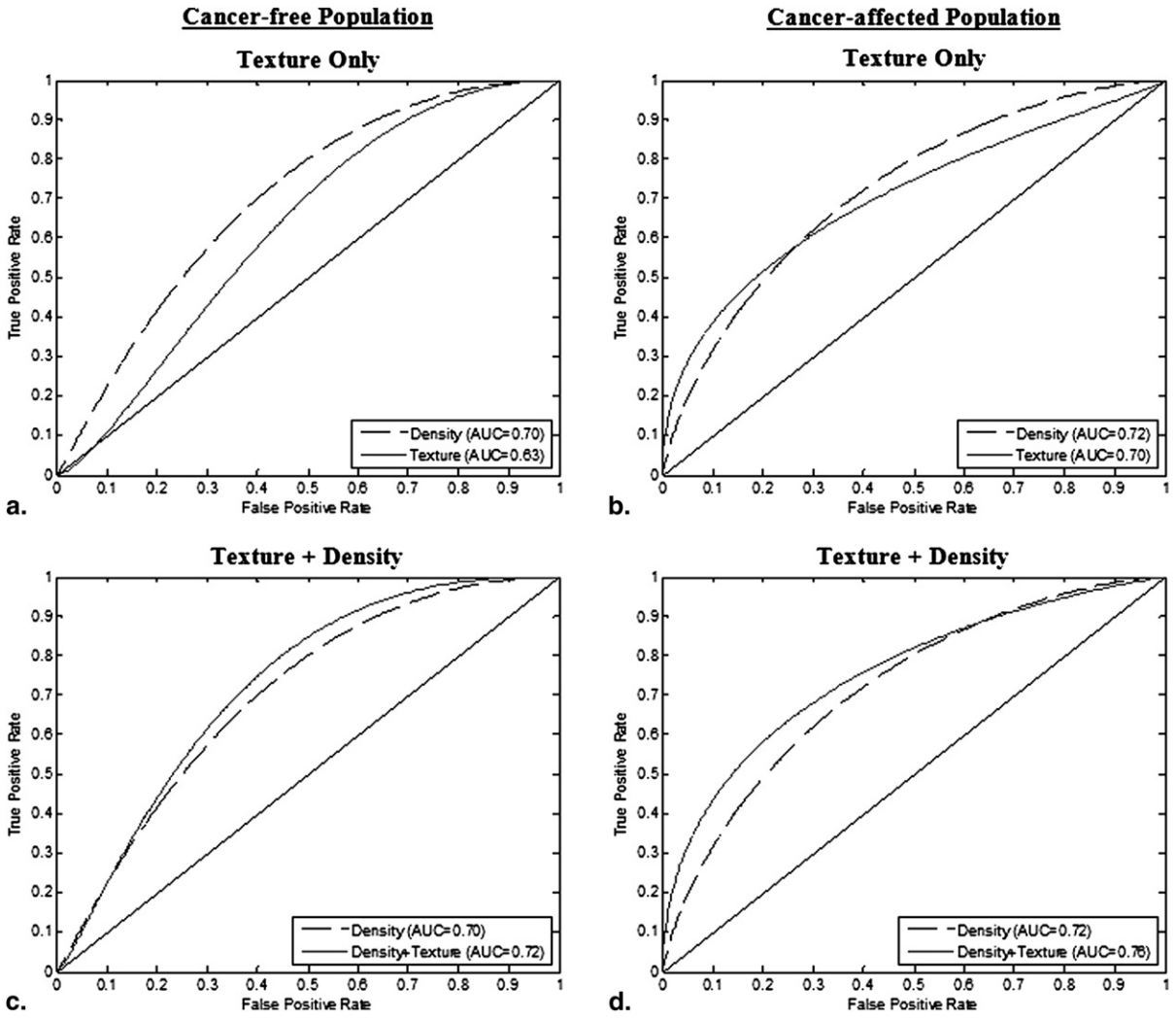

Figure 2. Receiver operating characteristic curves for logistic regression analysis for texture features only for the cancer-free **(a)** and cancer-affected women **(b)**; and texture features plus mammographic percent density for cancer-free **(c)** and cancer-affected women **(d)**. AUC, area under the curve. Data are shown for the models after backward feature selection.

texture features are associated to menopause status in the cancer-affected versus cancer-free women, suggesting that the breast tissue properties might be inherently different between these two populations. However, because of our relatively small sample set, these observations will need to be confirmed with larger clinical studies.

Our study has certain limitations. Designed as a preliminary evaluation, we chose to use menopause status as a surrogate for hormonal exposure. Although it is reasonable to assume that postmenopausal women have lower circulating estrogen levels when compared to premenopausal women, there is variability in the hormonal levels between women. A more rigorous measure of hormonal exposure could be used to more accurately assess hormonal levels in the blood (eg, serum estradiol levels) and correlate those directly with mammographic texture descriptors. In addition, our study population mainly consisted of a high-risk population, and therefore our findings will ultimately need to be validated in larger screening populations. Furthermore, texture analysis was confined within the retroareolar region of the breast. Although this area is thought to contain the most dense tissue and texturally complex portion of the breast (27), future work will seek to validate these findings using whole-breast texture analysis. Finally, we acknowledge that there are several potential additional texture features that we could have explored in this setting that may potentially capture additional tissue characteristics. Considering our sample size and issues of overfitting our models, we chose to use the most widely used and best validated texture features previously reported in the literature on breast cancer risk assessment. Our current study serves as a proof of concept; the inclusion and validation of additional texture features will constitute the subject of further investigations.

The research question currently actively investigated is to which extent parenchymal texture features can complement breast density in breast cancer risk estimation. To date, reports in the literature have shown mixed results. A study by Manduca et al (12) showed that parenchymal texture features in the low spatial frequencies are the strongest predictors of

risk and retain significance when breast density is considered; however, they do not significantly improve the ability to predict risk compared to breast density alone. In contrast, a recent study by Haberle et al (12) in a larger population showed that mammographic texture features can predict cancer risk with significant increase in model performance compared to density. Most studies to date have mainly used retrospective datasets from different patient populations and have used digitized film-screen mammograms (7,8,10,11,24,27,30) in which the effect of the film digitizer may have affected the predictive value of the computed image texture features. Studies with digital mammography offer the opportunity to fully explore the potential advantages of parenchymal texture analysis in breast cancer risk estimation by extracting quantitative features directly from the raw digital images. Larger prospective clinical studies are warranted to fully investigate the potential value of parenchymal texture analysis in breast cancer risk estimation.

CONCLUSION

Parenchymal texture has been previously associated with breast cancer risk. Yet, the biological basis of this association remains largely unknown. Here, we performed a study to assess parenchymal texture features as imaging markers of tissue hormonal exposure. Menopause status was used as a surrogate of endogenous hormonal activity. Our results suggest that certain mammographic texture features are significantly associated with menopause status. The observed association is stronger in cancer-affected women than cancer-free women and remains significant even when other hormonally related variables are considered, such as age at menarche, ethnicity, contraception use, estrogen therapy, parity, and age at first birth. Texture features may also contribute complementary information to that of mammographic density in reflecting tissue hormonal exposure. Parenchymal texture features could ultimately aid in breast cancer risk assessment as imaging markers of tissue hormonal exposure.

ACKNOWLEDGMENTS

We thank Dr. Johnny Kuo for developing and maintaining the Radiological Society of North America Medical Imaging Resource Center image archive as well as Ezra Bobo, Bethany Baumann, and Antonios Ioannou for their help with data collection and image analysis. We also thank Dr. Ahmed Ashraf for the useful discussions in statistical analysis. This work was partially supported by a Department of Defense Concept Award (BC086591), an American Cancer Society Research Scholar Grant (RSGHP-10-108-01-CPHPSAdd number), and a National Institutes of Health/National Cancer Institute Population0-based Research Optimizing Screening through Personalized Regimens Grant (1U54CA163313-01). D.D. is a Howard Hughes Medical Institute Gilliam Fellow.

REFERENCES

1. Armstrong K, Quistberg DA, Micco E, et al. Prescription of tamoxifen for breast cancer prevention by primary care physicians. Arch Intern Med 2006; 166:2260–2265.
2. Singh V, Saunders C, Wylie L, et al. New diagnostic techniques for breast cancer detection. Future Oncol 2008; 4:501–513.
3. Gulati AP, Domchek SM. The clinical management of BRCA1 and BRCA2 mutation carriers. Curr Oncol Rep 2008; 10:47–53.
4. Rockhill B, Spiegelman D, Byrne C, et al. Validation of the Gail et al. model of breast cancer risk prediction and implications for chemoprevention. J Natl Cancer Inst 2001; 93:358–366.
5. Tice JA, Cummings SR, Smith-Bindman R, et al. Using clinical factors and mammographic breast density to estimate breast cancer risk: development and validation of a new predictive model. Ann Intern Med 2008; 148:337–347.
6. Boyd NF, Martin LJ, Yaffe MJ, et al. Mammographic density and breast cancer risk: current understanding and future prospects. Breast Cancer Res 2011; 13:223.
7. Li H, Giger ML, Olopade OI, et al. Fractal analysis of mammographic parenchymal patterns in breast cancer risk assessment. Acad Radiol 2007; 14:513–521.
8. Huo Z, Giger ML, Olopade OI, et al. Computerized analysis of digitized mammograms of BRCA1 and BRCA2 gene mutation carriers. Radiology 2002; 225:519–526.
9. Caldwell CB, Stapleton SJ, Holdsworth DW, et al. Characterisation of mammographic parenchymal pattern by fractal dimension. Phys Med Biol 1990; 35:235–247.
10. Li H, Giger ML, Olopade OI, et al. Computerized texture analysis of mammographic parenchymal patterns of digitized mammograms. Acad Radiol 2005; 12:863–873.
11. Boyd NF, Guo H, Martin LJ, et al. Mammographic density and the risk and detection of breast cancer. N Engl J Med 2007; 356:227–236.
12. Manduca A, Carston MJ, Heine JJ, et al. Texture features from mammographic images and risk of breast cancer. Cancer Epidemiol Biomarkers Prev 2009; 18:837–845.
13. Haberle L, Wagner F, Fasching PA, et al. Characterizing mammographic images by using generic texture features. Breast Cancer Res 2012; 14: R59.
14. Chlebowski RT, McTiernan A. Biological significance of interventions that change breast density. J Natl Cancer Inst 2003; 95:4–5.
15. Greendale GA, Reboussin BA, Slone S, et al. Postmenopausal hormone therapy and change in mammographic density. J Natl Cancer Inst 2003; 95:30–37.
16. Prowell TM, Blackford AL, Byrne C, et al. Changes in breast density and circulating estrogens in postmenopausal women receiving adjuvant anastrozole. Cancer Prev Res (Phila) 2011; 4:1993–2001.
17. Clemons M, Goss P. Estrogen and the risk of breast cancer. N Engl J Med 2001; 344:276–285.
18. Kerlikowske K, Cook AJ, Buist DS, et al. Breast cancer risk by breast density, menopause, and postmenopausal hormone therapy use. J Clin Oncol 2010; 28:3830–3837.
19. Daye D, Bobo E, Baumann B, et al. Mammographic parenchymal texture as an imaging marker of hormonal activity: a comparative study between pre- and post-menopausal women. Medical Imaging 2011: Computer-Aided Diagnosis, Proc SPIE 2011;; 7963. 79631N–79631N.
20. Key T, Appleby P, Barnes I, et al. Endogenous sex hormones and breast cancer in postmenopausal women: reanalysis of nine prospective studies. J Natl Cancer Inst 2002; 94:606–616.
21. Missmer SA, Eliassen AH, Barbieri RL, et al. Endogenous estrogen, androgen, and progesterone concentrations and breast cancer risk among postmenopausal women. J Natl Cancer Inst 2004; 96:1856–1865.
22. Pike MC, Krailo MD, Henderson BE, et al. 'Hormonal' risk factors, 'breast tissue age' and the age-incidence of breast cancer. Nature 1983; 303: 767–770.
23. Grady D. Clinical practice. Management of menopausal symptoms. N Engl J Med 2006; 355:2338–2347.
24. Kontos D, Bakic PR, Carton AK, et al. Parenchymal texture analysis in digital breast tomosynthesis for breast cancer risk estimation: a preliminary study. Acad Radiol 2009; 16:283–298.
25. Kontos D, Ikejimba L, Bakic PR, et al. Digital breast tomosynthesis parenchymal texture analysis: comparison with digital mammography

and implications for cancer risk assessment. Radiology 2011; 261: 80–91.
26. Oliver A, Freixenet J, Marti R, et al. A novel breast tissue density classification methodology. IEEE Trans Inf Technol Biomed 2008; 12:55–65.
27. Kontos D, Ikejimba LC, Bakic PR, et al. Analysis of parenchymal texture with digital breast tomosynthesis: comparison with digital mammography and implications for cancer risk assessment. Radiology 2011; 261: 80–91.
28. Haralick RM, Shanmugam K, Dinstein I. Textural features for image classification. IEEE Trans Syst Man Cybernetics 1973; 3:610–621.
29. Amadasum M, King R. Textural features corresponding to textural properties. IEEE Trans Syst Man Cybernetics 1989; 19:1264–1274.
30. Wei J, Chan HP, Wu YT, et al. Association of computerized mammographic parenchymal pattern measure with breast cancer risk: a pilot case-control study. Radiology 2011; 260:42–49.
31. Huo Z, Giger ML, Wolverton DE, et al. Computerized analysis of mammographic parenchymal patterns for breast cancer risk assessment: feature selection. Med Phys 2000; 27:4–12.
32. Li H, Giger ML, Huo Z, et al. Computerized analysis of mammographic parenchymal patterns for assessing breast cancer risk: effect of ROI size and location. Med Phys 2004; 31:549–555.
33. McCormack VA, dos Santos Silva I. Breast density and parenchymal patterns as markers of breast cancer risk: a meta-analysis. Cancer Epidemiol Biomarkers Prev 2006; 15:1159–1169.
34. Keller B, Nathan D, Wang Y, et al. Adaptive multi-cluster fuzzy C-means segmentation of breast parenchymal tissue in digital mammography. Med Image Comput Comput Assist Interv 2011; 14: 562–569.
35. Keller BM, Nathan DL, Wang Y, et al. Estimation of breast percent density in raw and processed full field digital mammography images via adaptive fuzzy C-means clustering and support vector machine segmentation. Med Phys 2012; 39:4903–4917.
36. Brodersen KH, Ong CS, Stephan KE, et al. The binormal assumption on precision-recall curves. Proceedings of the 20th International Conference on Pattern Recognition (ICPR) 2010;4263–4266.
37. Pepe M, Longton G, Janes H. Estimation and comparison of receiver operating characteristic curves. Stata J 2009; 9:1.
38. Boyd N, Melnichouk O, Martin LJ, et al. Mammographic density, response to hormones, and breast cancer risk. J Clin Oncol 2011; 29:2985–2992.
39. Boyd N, Martin L, Stone J, et al. A longitudinal study of the effects of menopause on mammographic features. Cancer Epidemiol Biomarkers Prev 2002; 11:1048–1053.
40. Greendale GA, Reboussin BA, Sie A, et al. Effects of estrogen and estrogen-progestin on mammographic parenchymal density. Postmenopausal Estrogen/Progestin Interventions (PEPI) Investigators. Ann Intern Med 1999; 130:262–269.
41. Cuzick J, Warwick J, Pinney E, et al. Tamoxifen and breast density in women at increased risk of breast cancer. J Natl Cancer Inst 2004; 96:621–628.
42. Kontos D, Berger R, Bakic PR, et al. Breast tissue classification in digital breast tomosynthesis images using texture features: a feasibility study. In *SPIE Medical Imaging: Computer-Aided Diagnosis* M.L. Giger, and N. Karssemeijer, editors. Orlando, FL; 2009.
43. Raundahl J, Loog M, Pettersen P, et al. Automated effect-specific mammographic pattern measures. IEEE Trans Med Imaging 2008; 27: 1054–1060.
44. Haralick RM. Statistical and structural approaches to texture. Proc IEEE 1979; 67:786–804.
45. Li H, Giger ML, Olopade OI, et al. Power spectral analysis of mammographic parenchymal patterns for breast cancer risk assessment. J Digit Imaging 2008; 21:145–152.

APPENDIX

In this study, seven texture features were extracted from each region of interest (ROI). Skewness reflects the asymmetry of the gray-level histogram and has been used to assess parenchymal density (31,32). When the image texture is predominantly composed of fat (ie, the gray-level histogram is skewed to higher values), the skewness tends to be positive, whereas when the texture is primarily formed by dense tissue (ie, the gray-level histogram is skewed to lower values), the skewness values tend to be negative. Skewness is the third statistical moment, computed as:

$$skewness = \frac{w_3}{w_2^{\frac{3}{2}}} \quad where$$

$$w_k = \sum_{i=0}^{g_{\max}} n_i (i - \bar{i})^k / N, \quad N = \sum_{i=0}^{g_{\max}} n_i, \quad \bar{i} = \sum_{i=0}^{g_{\max}} (i n_i / N)$$

and n_i represents the number of times that gray level value i takes place in the image region, $g_{\max}$ is the maximum gray-level value, and N is the total number of image pixels.

Coarseness is a texture feature that reflects the local variation in image intensity; a small coarseness value for an ROI indicates fine texture, where the gray levels of neighboring pixels are different; a high coarseness value indicates coarse texture, where neighboring pixels have similar gray-level values. Coarseness computation is based on the Neighborhood Gray Tone Difference Matrix (NGTDM) (29) of the gray-level values within the image region.

$$coarseness = \left(\sum_{i=0}^{g_{\max}} p_i v(i) \right)^{-1}, \quad \text{where}$$

$$v(i) = \begin{cases} \sum |i - \overline{L}_i| \ for\ i \in \{n_i\}\ if\ \ n_i \neq 0 & \text{is the NGTDM} \\ 0 & otherwise \end{cases}$$

In the these formulas, g_{max} is the maximum gray-level value, p_i is the probability that gray level i occurs, n_i is the number of pixels having gray level value equal to i, and $\overline{L}_i$ is given by

$$\overline{L}_i = \frac{1}{S-1} \sum_{k=-t}^{t} \sum_{l=-t}^{t} j(x+k, y+l),$$

where $j(x,y)$ is the pixel located at (x,y) with gray level value i, $(k,l) \neq (0,0)$ and $S = (2d+1)^2$, with d specifying the neighborhood size around the pixel located at (x,y).

Contrast, energy, correlation, and homogeneity, as proposed originally by Haralick (28,44), require the computation of a gray-level cooccurrence matrix, which is based on the frequency of the spatial cooccurrence of gray-level intensities in the image. Contrast quantifies overall variation in image intensity, whereas energy is a measure of image homogeneity.

$$contrast = \sum_{i}^{g} \sum_{j}^{g} |\mathrm{i} - \mathrm{j}|^2 C(i,j),$$

$$energy = \sum_{i}^{g} \sum_{j}^{g} C(i,j),$$

$$correlation = \frac{\sum_i \sum_j (ij) p(i,j) - \mu_x \mu_y}{\sigma_x \sigma_y},$$

$$homogeneity = \sum_{i=0}^{g_{max}} \sum_{j=0}^{g_{max}} \frac{C(i,j)}{1 + |i-j|}$$

where g is the total number of gray levels, μ and σ are the mean and standard deviation of the partial probability density function p, and C is the normalized cooccurrence matrix (28,44).

Fractal dimension (FD) was estimated based on the power spectrum of the Fourier transform of the image (7,31,45). The two-dimensional (2D) discrete Fourier transform was performed using the fast Fourier transform algorithm as:

$$F(u,v) = \sum_{m=0}^{M-1} \sum_{n=0}^{N-1} I(m,n) e^{-j\left(\frac{2\pi}{M}\right)um} e^{-j\left(\frac{2\pi}{N}\right)vn},$$

$$u = 0, 1, \ldots, M-1 \quad v = 0, 1, \ldots, N-1$$

where I is the 2D image region of size (M, N), and u and v are the spatial frequencies in the x and y directions. The power spectral density P was estimated from $F(u,v)$ as:

$$P(u,v) = |F(u,v)|^2$$

To compute the FD, P was averaged over radial slices spanning the fast Fourier transform frequency domain. The frequency space was uniformly divided in 24 directions, with each direction uniformly sampled at 30 points along the radial component. To calculate the FD, the least-squares-fit of the $log(Pf)$ versus $log(f)$ was estimated, where $f = \sqrt{u^2 + v^2}$ denotes the radial frequency.

The FD is related to the slope β of this log-log plot by:

$$FD = \frac{3D_T + 2 - \beta}{2} = \frac{8 - \beta}{2}$$

where DT is the topological dimension, and is equal to 2 for a 2D image.